Analysis of Inositol Phosphate Metabolism by Capillary Electrophoresis Electrospray Ionization Mass Spectrometry (CE-ESI-MS)

Danye Qiu[a,*], Miranda S. Wilson[b], Verena B. Eisenbeis[a], Robert K. Harmel[c], Esther Riemer[d], Thomas M. Haas[a], Christopher Wittwer[a], Nikolaus Jork[a], Chunfang Gu[e], Stephen B. Shears[e], Gabriel Schaaf[d], Bernd Kammerer[a], Dorothea Fiedler[c], Adolfo Saiardi[b,*], Henning J. Jessen[a,f,*]

a) Institute of Organic Chemistry, University of Freiburg, Albertstr. 21, 79104 Freiburg, Germany
b) Medical Research Council, Laboratory for Molecular Cell Biology, University College London, London, WC1E 6BT, UK.
c) Leibniz-Forschungsinstitut für Molekulare Pharmakologie, Robert-Rössle-Str. 10, 13125 Berlin, Germany.
d) Institute of Crop Science and Resource Conservation, Department of Plant Nutrition, Rheinische Friedrich-Wilhelms-University Bonn, 53115 Bonn, Germany.
e) Signal Transduction Laboratory, National Institute of Environmental Health Sciences, National Institutes of Health, Research Triangle Park, NC 27709 USA
f) CIBSS - Centre for Integrative Biological Signalling Studies, University of Freiburg, 79104 Freiburg, Germany.

* danyeqiu@gmail.com; a.saiardi@ucl.ac.uk; henning.jessen@oc.uni-freiburg.de

Abstract

The analysis of *myo*-inositol phosphates (InsPs) and *myo*-inositol pyrophosphates (PP-InsPs) is a daunting challenge due to the large number of possible isomers, the absence of a chromophore, the high charge density, the low abundance, and the instability of the esters and anhydrides. Given their importance in biology, an analytical approach to follow and understand this complex signaling hub is highly desirable. Here, capillary electrophoresis (CE) coupled to electrospray ionization mass spectrometry (ESI-MS) is implemented to analyze complex mixtures of InsPs and PP-InsPs with high sensitivity. Stable isotope labeled (SIL) internal standards allow for matrix-independent quantitative assignment. The method is validated in wild-type and knockout mammalian cell lines and in model organisms. SIL-CE-ESI-MS enables for the first time the accurate monitoring of InsPs and PP-InsPs arising from compartmentalized cellular synthesis pathways, by feeding cells with either [$^{13}C_6$]-*myo*-inositol or [$^{13}C_6$]-D-glucose. In doing so, we uncover that there must be unknown inositol synthesis pathways in mammals, highlighting the unique potential of this method to dissect inositol phosphate metabolism and signalling.

Introduction

myo-Inositol (inositol hereafter) phosphates (InsPs) are second messengers involved in signaling processes in eukaryotes[1]. In principle, 63 phosphorylated InsPs can be generated by sequential phosphorylation of the hydroxy groups of inositol, resulting in significant

analytical ramifications. Moreover, the fully phosphorylated inositol hexakisphosphate $InsP_6$, the usually most abundant species, can be further phosphorylated to diphospho-inositol polyphosphates (PP-InsPs), called inositol pyrophosphates (Figure 1a and Supplementary Figure 1 for the mammalian PP-InsPs pathway)[2,3]. These structures contain one (PP-$InsP_5$) or two ($(PP)_2$-$InsP_4$) phosphoric anhydride (P-anhydride) bonds in addition to the phosphate esters (Figure1a). The current model for biologically relevant isomers places the P-anhydrides in defined positions. For example, mammals, yeast, and plants produce 5-PP-$InsP_5$ as the main isomer, with the P-anhydride residing in the plane of symmetry at the 5-position. The second, lower abundance, isomer is 1-PP-$InsP_5$, which has a biologically likely irrelevant enantiomer, its mirror-image 3-PP-$InsP_5$. Further phosphorylation of 5-PP-$InsP_5$ leads to 1,5-$(PP)_2$-$InsP_4$. PP-InsPs are considered metabolic messengers, whose functions have recently become the focus of intense research[4]. Across species, they are signals in diverse processes including the regulation of energy metabolism and phosphate homeostasis[5–7]. Other organisms, e.g. the social amoeba *Dictyostelium discoideum,* produce distinct PP-InsPs isomers (Figure1a) whose functions remain elusive[8,9].

The metabolic complexity of InsP turnover and their low abundance, in combination with the absence of a chromophore, and high charge density, has hampered research into these signaling molecules. The most widely applied quantification technology relies on metabolic labeling of cells using tritiated [^{3}H]-inositol, followed by acidic extraction, strong anion exchange high performance liquid chromatography (SAX-HPLC), and manual scintillation counting of individual fractions[10]. While this approach is sensitive, it requires a dedicated radioactive suite, is expensive, and labor and time-consuming. Moreover, it is blind to inositol generated endogenously from D-glucose-6-phosphate by inositol-3-phosphate synthase 1 (ISYNA1). Therefore, postcolumn derivatization UV-detection approaches have been developed to avoid radiolabeling[11,12]. Recently, it was shown that inositol tetrakisphosphate 1-kinase 1 (ITPK1), which is present in Asgard archaea, social amoeba, plants, and animals, sequentially phosphorylates Ins(3)P ultimately leading to $InsP_6$ and PP-InsPs[11,13,14]. Different InsP pools generated from exogenously-acquired or endogenously-synthesized inositol can potentially be monitored using chromatography coupled to mass spectrometry (LC-MS) after feeding cells with 'heavier' species such as [$^{13}C_6$]-inositol. However, standard SAX-HPLC using water-salt-based gradients is incompatible with MS detection and MS-compatible volatile buffers do not currently enable isomer assignment[15]. HPLC-MS/MS and hydrophilic interaction liquid chromatography coupled to MS (HILIC-MS/MS) unfortunately result in a suboptimal separation of the analytes, obliterating InsP isomer identity[16].

The development of resolving methods using an electric field to separate the differentially charged InsPs has been pursued. High-voltage paper chromatography[17] was instrumental in the discovery and establishment of Ins(1,4,5)P_3 as the Ca^{2+} release factor[18]. The separation

of higher InsPs by gel electrophoresis (PAGE) is another possibility; it, however, does not have the resolving power to distinguish PP-InsP regioisomers and does not detect lower InsPs due to staining inefficiency[19].

A capillary electrophoresis (CE) mass spectrometry (MS) method is described herein, that complements and significantly improves analytical approaches in the field. It does not require derivatization, benefits from the separation efficiency of charged analytes by CE, and enables accurate isomer identification and quantification using stable isotope labeled (SIL) reference compounds, even in complex matrices. This new setup also enables stable isotope pulse labeling experiments to analyze the amount of endogenously synthesized inositol over time.

Results

Development of CE-ESI-MS for the analysis of InsPs and PP-InsPs

CE is known as an effective separation tool for phosphate-containing molecules. An early attempt to implement CE was made in the study of Ins(1,4,5)P_3, but the method was not developed further[20]. We now introduce a CE-ESI-MS method, using a bare fused silica capillary and a simple background electrolyte (BGE), for parallel analyses of PP-InsPs and InsPs.

A set of PP-InsP and InsP standards (Figure 1b), representing mammalian metabolites (Figure 1a, Supplementary Figure 1), including Ins(1,4,5)P_3, Ins(1,3,4,6)P_4, Ins(1,4,5,6)P_4, Ins(1,3,4,5)P_4, Ins(2,3,4,5,6)P_5, Ins(1,3,4,5,6)P_5, Ins(1,2,3,4,6)P_5, Ins(1,2,3,4,5)P_5, InsP_6, 5-PP-InsP_5, 1-PP-InsP_5, and 1,5-$(PP)_2$-InsP_4, was resolved with a BGE (35 mM ammonium acetate adjusted to pH 9.7 with NH_4OH) by applying a 30 kV voltage over a regular bare fused silica capillary with a length of 100 cm. Detection of analytes was achieved with an ESI-TOF-MS instrument in the negative ionization mode. A stable CE separation current (23 µA) and ESI spray current (2.1 µA) were maintained with a sheath flow CE-ESI-MS interface. The limits of quantification (LOQs) for different InsPs were 250 nM, with 10 nL sample injection volume, i.e. 2.5 fmol of analyte. As baseline separation for the analytes is achieved, no issues with the inevitable in-source fragmentation with neutral loss of phosphate are encountered for accurate quantification. Generally, less than 10% in-source fragmentation products were produced from doubly charged anionic forms of InsP_5 to InsP_8 with neutral loss of phosphate (79.97 Da).

Next, we validated the CE-ESI-MS protocol in analyzing InsPs from biological samples. Initially, we focused on two HCT116 cell lines ($HCT116^{UCL}$ and $HCT116^{NIH}$) that have been shown to possess different PP-InsP levels[21]. The CE-ESI-MS method was fully compatible with current state-of-the-art InsP extraction by perchloric acid followed by enrichment with TiO_2 (Figure 1c). We introduced and resolved in parallel stable-isotope labelled (SIL) internal standards of [$^{13}C_6$]1,5-$(PP)_2$-InsP_4, [$^{13}C_6$]5-PP-InsP_5, [$^{13}C_6$]1-PP-InsP_5, [$^{13}C_6$]InsP_6 and [$^{13}C_6$]Ins(1,3,4,5,6)P_5[22]. Application of SIL standards is crucial, as the assignment of InsPs,

particularly regioisomers, now becomes unambiguous. Spiking with precise amounts of SIL standards into a biological extract also enables a reliable quantitative assessment, since they compensate for matrix effects and analyte loss. Ins(1,3,4,5,6)P_5, InsP_6, and 5-PP-InsP_5 were assigned by their isotopic pattern, accurate mass, and identical migration time with spiked SIL standards. Excellent resolution and column efficiency were obtained: 1.5×10^4, 4.6×10^4, 3.0×10^4 theoretical plates per meter for 5-PP-InsP_5, InsP_6 and Ins(1,3,4,5,6)P_5, isolated from HCT116^{NIH} extract, respectively (Figure 1c). Analysis of HCT116^{UCL} extract found 1,5-$(PP)_2$-InsP_4 (Figure 2aI), a signal which was generally under the LOQ (250 nM) but within LOD in HCT116^{NIH} extract (Figure 2aII), consistent with previous observations[21]. Furthermore, the analysis of HCT116^{UCL} confirmed the presence of the less abundant 1-PP-InsP_5 isomer, representing less than 10% of the cellular PP-InsP pool (Figure 2aIII). This is an important step forward for characterizing PP-InsP metabolism using mass spectrometry. The TiO_2 extraction method was previously reported to fully recover PP-InsPs and InsP_6 from mammalian cell extracts[23]. We confirmed this observation by spiking the HCT116^{NIH} samples with SIL internal standards both before extraction (pre-spiking) and before measurement (post-spiking) (Supplementary Figure 2).

The CE-ESI-MS protocols are not limited to analysis of InsP_6 and PP-InsPs. Using the described conditions, Ins(1/3,2,4,5,6)P_5 and Ins(1,2,3,4,6)P_5 or Ins(1,2,3,4/6,5)P_5 were readily distinguished from Ins(1,3,4,5,6)P_5 (Supplementary Figure 3a). Similarly, identification of InsP_4 positional isomers was achieved by measuring the accurate mass in combination with spiking of InsP_4 standards Ins(1,3,4,6)P_4, Ins(1,4,5,6)P_4 and Ins(1,3,4,5)P_4 (Figure 2b).

Owing to minimal sample consumption (10 nL) and rapid analysis time (30 min) per run, measurement of technical replicates is feasible. The intra- and inter-day repeatabilities of the method analyzing HCT116^{NIH} extract were evaluated, with mean RSDs of 3.0% (Day 1), 3.1% (Day 2) and 6.3% (Day 3) for three technical replicates, and a mean RSD of 3.6% for technical replicates from five individual days (Figure 1d). A comparison with the repeatabiliy of SAX-HPLC studies is difficult: details of technical replicates are often not provided, since the analysis of one sample takes about 6-8 hours with hands-on processing[24,25].

CE-ESI-MS analysis of mammalian PP-InsP metabolism

The CE-ESI-MS method was also applied to monitor changes in PP-InsPs metabolism in mammalian cells in which their synthetic enzymes have been knocked out or perturbed using inhibitors. In mammals, PP-InsPs are synthesized by two different classes of enzymes (Supplementary Figure 1). The IP6Ks, by phosphorylating position 5 of InsP_6, synthesize 5-PP-InsP_5. The PPIP5Ks are bifunctional (kinase/phosphatase) enzymes that, by acting on position 1, mainly convert 5-PP-InsP_5 into 1,5-$(PP)_2$-InsP_4. CE-ESI-MS analysis of

HCT116^{UCL}*IP6K1,2*$^{-/-}$ confirms prior observations that PP-InsPs are absent (Figure 2aV)[26]. Levels of PP-InsPs can be increased by blocking their dephosphorylation using sodium fluoride (NaF, 10 mM)[27]. CE-ESI-MS analysis of NaF-treated HCT116^{UCL} (Supplementary Figure 3) or HCT116^{NIH} cells (Figure 2c) demonstrated the expected 5-PP-InsP$_5$ elevation (7.3-fold in HCT116^{UCL} cells and 6.2-fold in HCT116^{NIH} cells) with concomitant reduction in InsP$_6$. We observed a reduction in Ins(1,3,4,5,6)P$_5$ levels and appearance of 5-PP-InsP$_4$ (Figure 2aIV), changes also observable by SAX-HPLC analysis of [^{3}H]-inositol labeled HCT116^{UCL} (Supplementary Figure 3). The synthesis of 5-PP-InsP$_4$ is dependent on IP6Ks acting on Ins(1,3,4,5,6)P$_5$: consistent with this, CE-ESI-MS analysis of NaF-treated HCT116^{UCL}*IP6K1,2*$^{-/-}$ also failed to detect any 5-PP-InsP$_4$. However, confirming a previous observation[26], 1-PP-InsP$_5$ became detectable in HCT116^{UCL}*IP6K1,2*$^{-/-}$ after NaF treatment (Figure 2aVI). This is explained by PPIP5Ks' capacity to use InsP$_6$ as a substrate, particularly when its preferred substrate, 5-PP-InsP$_5$, is absent. We also observed an increase in Ins(1/3,4,5,6)P$_4$ levels in NaF-treated HCT116^{NIH} cells (Figure 2b) as a result of PLC activation[27]. Analysis of HCT116^{NIH}*PPIP5K1,2*$^{-/-}$ in comparison to WT cells showed a small increase of the non-metabolized substrate 5-PP-InsP$_5$, the levels of which are 3.6-fold enhanced by NaF treatment (Figure 2c). We additionally analyzed the effect of a recently identified IP6K inhibitor: quercetin (Q)[28] reduced 5-PP-InsP$_5$ levels in both HCT116^{NIH} and HCT116^{NIH}*PPIP5K1,2*$^{-/-}$ cells by 50-60% (Figure 2c).

These results validate CE-ESI-MS as a technique to monitor with unprecedented accuracy changes in cellular InsPs and PP-InsPs metabolism in response to different stressors or genetic alterations.

Analysis of InsPs in mammalian cell lines and tissues

We determined the concentrations of Ins(1,3,4,5,6)P$_5$, InsP$_6$, and 5-PP-InsP$_5$, in different mammalian cell lines, including HCT116^{UCL}, HeLa, HT29, PC3, 293T, and MCF7 (Figure 2d, Supplementary Figure 4). The detected InsP$_6$ and 5-PP-InsP$_5$ cellular concentrations as well as their relative ratio are in accordance with earlier results obtained by [^{13}C]-NMR[29]. The InsP$_6$ cellular concentration, for example, was in the range of 24-47 µM (300-500 pmol/mg protein). However, Ins(1,3,4,5,6)P$_5$ levels were surprisingly variable, potentially reflecting different functional roles (Supplementary Figure 5) across different cell lines. Therefore, the CE-MS method will be instrumental to uncover dynamics and physiological roles of InsP$_5$ in mammalian cells.

We quantified the amount of InsPs and PP-InsPs in mouse organs, including liver, brain, muscle, kidney, and spleen (Supplementary Figure 6). Again, Ins(1,3,4,5,6)P$_5$, InsP$_6$, and 5-PP-InsP$_5$ were the main InsP species. Comparably low InsP levels were detected in muscle. Analysis of InsP$_6$ and 5-PP-InsP$_5$ extracted from tissues performed by PAGE, lack the

sensitivity, resolution and dynamic range, evidenced by CE-ESI-MS. The analysis of InsPs from animal organs or tissues cannot be performed by SAX-HPLC, prohibited by cost, feasibility, and ethical considerations, since it requires feeding a mouse with [^{3}H]-inositol.

InsPs and PP-InsPs in *Saccharomyces cerevisiae* and *Arabidopsis thaliana*

We next analyzed InsPs and PP-InsPs in yeast and plant samples, to explore the applicability of CE-ESI-MS across experimental models. The [^{3}H]-inositol SAX-HPLC method has been extensively employed to study yeast and plant InsP metabolism. PAGE methods conversely cannot be used to analyze InsPs from yeast, due to the abundant inorganic polyphosphate (polyP) that suppresses the InsP signals (Supplementary Figure 7a), and while PAGE has been applied to study InsPs including PP-InsPs in plant extracts[14,30,31], the same limitations described above apply. Using SIL-CE-ESI-MS, profiling of InsPs and PP-InsPs was readily achieved for both *Saccharomyces cerevisiae* and *Arabidopsis thaliana*.

In wild type yeast extracts, $InsP_6$, 5-PP-$InsP_5$ and 1/3,5-$(PP)_2$-$InsP_4$ were detectable. In agreement with the literature[32], 5-PP-$InsP_5$ and 1/3,5-$(PP)_2$-$InsP_4$ were around 3% and 1% of the $InsP_6$ level, respectively (Supplementary Figure 7).

We analyzed the InsPs present in shoots of *A. thaliana* wild type (Col-0) and in plants defective in Inositol Pentakisphosphate 2-Kinase (AtIPK1) or the ATP-binding cassette (ABC) transporter 5 (AtMRP5)[33] that transports $InsP_6$ into the vacuole (Figure 3): Ins(1/3,2,4,5,6)P_5, $InsP_6$, 5-PP-$InsP_5$, 1/3-PP-$InsP_5$ and 1/3,5-$(PP)_2$-$InsP_4$ were readily detected in shoot extracts of *A. thaliana* Col-0 seedlings. Surprisingly, comparable levels of 5-PP-$InsP_5$ and 1/3-PP-$InsP_5$ were observed. This represents a significant deviation from the general notion, derived from mammalian cell analysis, that 1-PP-$InsP_5$ represents the minor isomeric species. The *atipk1* mutant displayed decreased levels of PP-InsPs and $InsP_6$, and a robust increase in Ins(1,3,4,5,6)P_5 s. In *atipk1* plants, 5-PP-$InsP_4$ was also detected by CE-ESI-MS, which was previously unsuccessfully tracked by [^{3}H]-inositol labelling and SAX-HPLC analysis[34]. Analysis of *atmrp5* shoots revealed the expected elevated levels of 5-PP-$InsP_5$ and 1/3,5-$(PP)_2$-$InsP_4$, but not of 1/3-PP-$InsP_5$. This analysis represents the first detailed elucidation of single isomer PP-InsP alterations in plants, underlining the value of the SIL-CE-ESI-MS method for dissecting PP-InsP isomers and relative abundances.

CE-ESI-MS to analyze *Dictyostelium discoideum* PP-InsP metabolism

The social amoeba *Dictyostelium discoideum* possesses large amounts of PP-InsPs. However, this model organism contains different PP-InsPs isomers from those in mammals, yeast and plants, such as 6-PP-$InsP_5$ and 5,6-$(PP)_2$-$InsP_4$[9,35]. This complexity is a challenge for ideal CE separation conditions. Employing a different BGE with decreased ionic strength and pH (30 mM ammonium acetate adjusted to pH 9.0 with NH_4OH) led to enhanced resolution

of $InsP_6$ and more anionic species. Under these conditions, all possible PP-$InsP_5$ isomers, including non-natural ones obtained by chemical synthesis[36–38], were separated and could thus be assigned in complex matrices (Figure 4a). This BGE also enabled the separation of all available $InsP_5$ isomers. We then performed CE-ESI-MS analyses of *D. discoideum* extracts (Figure 4b). As expected, 4/6-PP-$InsP_5$ was about twice as abundant as 5-PP-$InsP_5$, while 1/3-PP-$InsP_5$ was present at around 5% of the whole PP-$InsP_5$ pool. We identified two $(PP)_2$-$InsP_4$ isomers, 5,4/6-$(PP)_2$-$InsP_4$, and 1,5-$(PP)_2$-$InsP_4$. Peak assignment and quantification were conducted in a single run (30 minutes), and accurate mass information was provided simultaneously (Figure 4c).

Endogenous inositol synthesis contributes to the InsP pools

The ability of MS to capture isotopic mass differences is a significant advantage of the CE-ESI-MS protocol. For example, by using isotopically labeled metabolic precursors, the contribution to the InsP pool of both the inositol acquired from the milieu and from endogenous synthesis from glucose can now be assessed (Figure 1a). In SAX-HPLC analysis, inositol-free medium is used to improve [^{3}H]-inositol labeling, with the tracer used at 0.5-1 µM concentration[25]. This method does not detect endogenously generated inositol. To assess the contribution of endogenous synthesis of inositol to InsP cellular pools, we performed an inositol titration curve. Wild type HCT116^{UCL} were incubated for five days, the incubation time used for [^{3}H]-inositol labeling to reach metabolic equilibrium (7-8 cell division cycles), in inositol-free DMEM in the presence of 1, 10 and 100 µM [$^{13}C_6$]-inositol. We observed a dose-dependent incorporation of [$^{13}C_6$]-inositol into the [$^{13}C_6$]$InsP_5$ and [$^{13}C_6$]$InsP_6$ pools (Figure 5a). Using 1 µM [$^{13}C_6$]-inositol, less than 20% of the $InsP_5$ and $InsP_6$ pools were synthesized from exogenously acquired inositol; this value increased to 90% using 100 µM. A reference value for inositol concentration in human serum is 30 µM[39], available only to cells in direct contact with serum. We next performed a time course, incubating cells with [$^{13}C_6$]-inositol (10 µM) in inositol-free DMEM for 1, 3 and 5 days (Figure 5b). Initially, all $InsP_5$ and $InsP_6$ species were constituted of [^{12}C]-inositol. By 24 h [$^{13}C_6$]$InsP_5$ and [$^{13}C_6$]$InsP_6$ became detectable, representing a small fraction of their respective pools. After five days, [$^{13}C_6$]$InsP_5$ and [$^{13}C_6$]$InsP_6$ represented two thirds of the $InsP_5$ and $InsP_6$ pools. These results indicate either a sluggish $InsP_5$ and $InsP_6$ turnover, even more lethargic than previously thought[40], or an endogenous synthesis of [^{12}C]-inositol that substantially contributes to the $InsP_5$ and $InsP_6$ pools.

The inositol phosphate synthase (IPS or MIPS) called ISYNA1 in mammals converts glucose-6-phosphate to Ins(3)P[41]. To study the contribution of endogenous inositol synthesis to InsP pools, we generated two independent HCT116^{UCL} *ISYNA1*$^{-/-}$ clones using CRISPR. The two knockout clones, KO1 and KO2, were verified by sequencing (Supplementary Figure 8) and

western blot analysis (Figure 6a). The $InsP_6$ level as analyzed by PAGE was unaffected in the *ISYNA1*$^{-/-}$ clones (Figure 6b), and there was no growth defect in normal medium (Figure 6c). Titrating the medium with different inositol concentrations revealed 10 µM inositol as sufficient to guarantee wild type growth rate, while the absence of inositol dramatically reduced the growth of both clones (Figure 6d-f). To study the contribution of ISYNA1 to the InsP pools, we incubated wild type HCT116^{UCL} and *ISYNA1*$^{-/-}$ clones for 5 days in 25 mM [$^{13}C_6$]-glucose with 1 or 10 µM inositol, and then extracted and analyzed the samples by CE-ESI-MS (Figure 6g). In wild type cells with only 1 µM inositol, roughly 60% of the $InsP_5$ and $InsP_6$ pools were generated by the endogenous conversion of [$^{13}C_6$]-glucose-6-phosphate to Ins(3)P, detected as [$^{13}C_6$]$InsP_5$ and [$^{13}C_6$]$InsP_6$. Note that often 1 µM or less of inositol is used in [^{3}H]-inositol labeling for SAX-HPLC experiments[26,42]. Our analysis, therefore, reveals that up to 60% of InsPs are not detected by traditional methods if inositol concentration is kept low to improve [^{3}H]-inositol labeling efficiency. In the presence of a tenfold higher exogenous inositol concentration (10 µM), endogenously generated inositol contributed 15% to the $InsP_5$ and $InsP_6$ pools. Strikingly, we detected [$^{13}C_6$]$InsP_5$ and [$^{13}C_6$]$InsP_6$ in both *ISYNA1*$^{-/-}$KO1 and *ISYNA1*$^{-/-}$KO2, although to a lesser extent than in wild type cells (Figure 6h-j). This highly unexpected result indicates the existence of an alternative uncharacterized enzymology for inositol synthesis, underscoring the enormous potential of the CE-ESI-MS technique. This approach will be instrumental not only in elucidating the novel inositol synthetic route we have discovered, but also in any future assessment of inositol phosphate physiological functions across the kingdoms of life.

Discussion

The analysis of InsP and PP-InsP turnover in cells and tissues is a daunting challenge. Radiolabeling followed by SAX-HPLC has so far been the method of choice, as it provides the sensitivity needed for meaningful analyses of the less abundant species, with the advantage of selectively visualizing only InsPs and PP-InsPs when [^{3}H]-labeled inositol is fed to cells. This approach, however, misses inositol endogenously synthesized from glucose, is restricted to specialized laboratories, is expensive, and time-consuming. While other approaches, such as [^{13}C] labeling for NMR, PAGE, and HILIC-MS, have recently been developed to provide alternatives, a transformative approach is still missing.

Here, we have demonstrated that CE is an outstanding separation platform for InsPs and PP-InsPs. Moreover, CE coupling to an ESI-Q-TOF mass spectrometer facilitates parallel analyses of a multitude of analytes in a single run, requiring only 30 minutes and nL sample injection. According to the accurate mass information and identical mobility with (isotopic) standards, these densely charged species can now be readily assigned even in complex matrices. Additionally, the introduction of stable isotope labeled (SIL) reference compounds

allows for quantification and correction of matrix effects in samples such as those obtained from yeast extracts rich in polyphosphates, where drifts in migration times of several minutes were observed. Using this approach, we were able to quantify InsPs and PP-InsPs in different species, and in wild type and knock-out cell lines additionally treated with inhibitors of several enzymes. Given the rapidity of the analysis, measurement of technical replicates becomes possible, underlining the robustness and fidelity of the method. Using CE-ESI-MS, we have been able to extract essential new information from several samples. For example, Ins(1,3,4,5,6)P_5 concentrations are highly variable across different mammalian cell lines and whole organs. We also show that 1/3-PP-InsP_5 is not always the minor isomer present, as exemplified by our analysis of *A. thaliana* seedlings, raising questions concerning its potential regulatory effects. Moreover, SIL inositol and SIL D-glucose were used in pulse labeling experiments, demonstrating that SIL-CE-ESI-MS can be used to monitor and quantify inositol isomer turnover originating from different sources. At low (1 µM) exogenous inositol concentration, around 60% of cellular inositol was derived from glucose after 5 days of labeling. Yet, knockout of the only known glucose-6-phosphate utilizing inositol synthase in mammalian cells (ISYNA1) did not lead to cells incompetent in transforming D-glucose to inositol. This finding reveals that there must exist a yet uncharacterized biochemical pathway for the synthesis of inositol deriving its carbon skeleton from glucose. We thus conclude that SIL-CE-ESI-MS will open our eyes to cellular pathways we have previously been blind to.

Methods

Materials and Reagents

InsP_6, Ins(1,3,4,5,6)P_5, Ins(2,3,4,5,6)P_5, Ins(1,2,3,4,6)P_5, Ins(1,2,3,4,5)P_5, Ins(1,3,4,5)P_4 and Ins(1,4,5)P_3 with purity more than 95-97% ([^{31}P] NMR) were purchased from Sichem. Ins(1,3,4,6)P_4 and Ins(1,4,5,6)P_4 were obtained from Cayman. 1-PP-InsP_5, 5-PP-InsP_5, 6-PP-InsP_5 and 2-PP-InsP_5 were synthesized in-house (Jessen)[36–38]. Stable-isotope labelled (SIL) internal standards [$^{13}C_6$]1,5-$(PP)_2$-InsP_4, [$^{13}C_6$]5-PP-InsP_5, [$^{13}C_6$]1-PP-InsP_5, [$^{13}C_6$] InsP_6, and [$^{13}C_6$]Ins(1,3,4,5,6)P_5 with purities higher than 96% were synthesized in-house (Fiedler)[22,29]. Concentrations of stock solutions of InsP and PP-InsP standards for quantification were determined by [^{1}H] NMR and/or [^{31}P] NMR as described below. Fused silica capillaries were obtained from CS-Chromatographie.

CE-ESI-MS Analysis

All experiments were performed on a bare-fused silica capillary with a length of 100 cm (50 µm internal diameter and 365 µm outer diameter) on an Agilent 7100 capillary electrophoresis system coupled to a Q-TOF (6520, Agilent) equipped with a commercial CE-MS adapter and

sprayer kit from Agilent. Prior to use, the capillary was flushed for 10 min with 1N NaOH, followed by water for 10 min, and background electrolyte (BGE) for 15 min. BGE A (35 mM ammonium acetate titrated by ammonia solution to pH 9.7) was employed for the analysis of all mammalian cell and tissue extracts, as well as *Saccharomyces cerevisiae* and *Arabidopsis thaliana* extracts. BGE B (30 mM ammonium acetate titrated by ammonia solution to pH 9.0) was used for *Dictyostelium discoideum*. Samples were injected by applying 50 mbar pressure for 10 s, corresponding to 0.5% of the total capillary volume (10 nL). In the study of the endogenous inositol synthesis, samples were injected with 100 mbar pressure for 10 s (20 nL). After sample injection, a BGE post-plug was introduced by applying 50 mbar for 2 s. For each analysis, a constant CE current of either 23 µA (BGE A) or 19 µA (BGE B) was established by applying 30 kV over the capillary, which was kept at a constant temperature of 25 °C.

The sheath liquid was composed of a water-isopropanol (1:1) mixture spiked with mass references. It was introduced at a constant flow rate of 1.5 µL/min. ESI-TOF-MS was conducted in the negative ionization mode; the capillary voltage was set to -3000 V and stable ESI spray current at 2.1 µA. For TOF-MS, the fragmentor, skimmer, and Oct RFV voltage was set to 140, 60, and 750 V, respectively. The temperature and flow rate of drying gas was 250 °C and 8 L/min, respectively. Nebulizer gas pressure was 8 psi. Automatic recalibration of each acquired spectrum was performed using reference masses of reference standards (TFA anion, $[M-H]^-$, 112.9855), and (HP-0921, $[M-H+CH_3COOH]^-$, 980.0163). Exact mass data were acquired at a rate of 1.5 spectra/s over a 60−1000 *m/z* range. Extracted ion electropherograms (EIEs) were created using a 10 ppm mass tolerance window for theoretical masses corresponding to the targeted inositol pyrophosphates and inositol phosphates.

Peak assignment of 1/3,5-$(PP)_2$-$InsP_4$, 5-PP-$InsP_5$, 1/3-PP-$InsP_5$, $InsP_6$ and Ins(1,3,4,5,6)P_5 in biological samples was achieved by accurate mass, isotopic pattern, and identical migration time. Ins(1,3,4,6)P_4, Ins(1/3,4,5,6)P_4 and 4/6-PP-$InsP_5$ in biological samples were assigned by accurate mass and identical migration time with spiked standards. 5-PP-$InsP_4$ and 4/6,5-$(PP)_2$-$InsP_4$ in biological samples were assigned by accurate mass and based on previous research[9,26].

Quantification of PP-InsP and InsP in mammalian cells was performed with known amounts of individual isotopic standards spiked into the samples. The amount of isotopic internal standards (IS) that had to be added was delineated from the concentration of the respective analyte in the sample. Ratio of analyte peak area $(Area)^{12C}$/ IS peak area $(Area)^{13C}$ is less than 5 to ensure a linear relationship. IS stock solutions of 125 µM [$^{13}C_6$]5-PP-$InsP_5$, 500 µM [$^{13}C_6$]$InsP_6$ and 500 µM [$^{13}C_6$]Ins(1,3,4,5,6)P_5 were used for the spiking experiments. 0.4 µL IS stock solution were added into 10 µL samples before measurement. 5 µM [$^{13}C_6$]5-PP-$InsP_5$, 20 µM [$^{13}C_6$]$InsP_6$ and 20 µM [$^{13}C_6$]Ins(1,3,4,5,6)P_5 were the final concentrations inside

klsamples. The calibration curve for each analyte was constructed at eight levels by regression of nominal analyte concentration against a ratio of analyte peak area (Area)^{12C}/ IS peak area (Area)^{13C} (Supplementary Figure 9). The calibration curves were linear and provided a coefficient of determination >0.997 over the investigated range of concentrations (0.25-25 µM for 5-PP-InsP_5, 1.0-100 µM for InsP_6 and Ins(1,3,4,5,6)P_5). For quantification, two technical replicates were conducted for each sample.

Quantification of InsP and PP-InsP in tissue extracts, *Saccharomyces cerevisiae, Arabidopsis thaliana,* and *Dictyostelium discoideum* extracts was performed by comparing analyte peak areas with the respective peak areas of SIL internal standards with known concentrations. Concentrations of SIL internal standard solutions were determined by quantitative ^{31}P and ^{1}H NMR against a certified reference standard (phosphoacetic acid, *Trace*CERT® Merk 96708-1G).

Maintenance and manipulation of mammalian cell lines

HCT116^{NIH} and HCT116^{NIH} *PPIP5K*$^{-/-}$ cells[43] were grown in DMEM (Gibco) supplemented with 4.5 g/L glucose and 10 % heat inactivated FBS (Gibco). HCT116^{UCL} (obtained from European Collection of Authenticated Cell Cultures [ECACC]) and HCT116^{UCL} *IP6K1,2*$^{-/-}$ cells[44] were cultured in DMEM supplemented with 10% FBS (Sigma) and 4.5 g/L glucose. All cells were grown in a humidified atmosphere with 5% CO_2. InsP levels were modulated by incubating the cells for 60 min with 10 mM NaF or for 30 min with 2.5 µM quercetin[28] prior to harvesting.

For inositol limitation or [$^{13}C_6$]-inositol labelling experiments, inositol-free DMEM (MP Biomedicals) with 10% dialyzed FBS (Sigma) was used. Normal inositol (Sigma) or [$^{13}C_6$]-inositol[29] were supplemented as appropriate. Cells were acclimatized to 10 µM inositol in inositol-free DMEM for one week before starting labelling experiments. For [$^{13}C_6$]-glucose (Sigma) labelling experiments, DMEM lacking both inositol and glucose (Thermo Fisher) was used, using 10% dialyzed FBS. Cells were washed twice in the relevant starvation medium before incubation.

Mammalian cell growth assay

To measure cell growth, the sulforhodamine B (SRB) assay was performed[45]. Cells were seeded into 96 well plates. After 24 h, the medium was removed, wells were washed, then 100 µL treatment medium was added. At each timepoint, cells were fixed in 10% trichloroacetic acid. Fixed plates were stained with 0.05% sulforhodamine B (Sigma) in 1% acetic acid, and fixed dye was solubilised in 10 mM Tris base before reading absorbance at 500 nm using a spectrophotometer.

To measure cell volume, 80-90% confluent cells were trypsinised and resuspended in growth medium. A Multisizer 4 (Beckman Coulter) machine was used, following the manufacturer instruction.

Generation of ISYNA1 KO cell lines

The human colon carcinoma cell line HCT116 was used to generate knockouts as it is pseudo-diploid, and has easily detectable amounts of $InsP_6$ and $InsP_7$[23]. The Alt-R CRISPR-Cas9 (Integrated DNA Technologies) system was used, with guide sequence 5'-CCAAUCGACUGCGUU-3'. CRISPR components were introduced into the cells using a Neon electroporator (Thermo Fisher) and cells plated into 96 well plates using limiting dilution. Colonies were screened by western blotting using anti-ISYNA1 antibody (Santa Cruz sc-271830). Positive knockout clones were further confirmed by PCR and Sanger sequencing-based analysis (Genewiz CRISPR Analysis Package).

Purification of inositol phosphates by titanium dioxide pulldown

Extraction of inositol phosphates was performed according to the literature[44]. Briefly, 80-90% confluent cells were extracted using 1 M perchloric acid as described below. Titanium dioxide beads (Titansphere TiO 5 µm; GL Sciences) were used to pull down inositol phosphates, which were eluted using 3% ammonium hydroxide. The ammonia was eliminated and the samples concentrated using a speedvac evaporator for 1-3 h at 40°C or 60°C. For InsPs analysis by PAGE, the extracts were normalized to protein concentration and resolved using 35% PAGE gels, as previously described[19]. Inositol phosphates were visualized by Toluidine blue (Sigma) staining. A desktop scanner (Epson) was used to record the PAGE result.

Preparing cell extracts for CE-ESI-MS

Mammalian cells:

Cells (8 million $HCT116^{UCL}$ cells, $HCT116^{UCL}$ *IP6K1,2*$^{-/-}$ cells and $HCT116^{NIH}$ *PPIP5K*$^{-/-}$ cells; 6 million $HCT116^{NIH}$ cells) were seeded into 15 cm dishes and allowed to grow for 48 hours ($HCT116^{UCL}$ and $HCT116^{UCL}$ *IP6K1,2*$^{-/-}$ cells) or 72 hours ($HCT116^{NIH}$ and $HCT116^{NIH}$ *PPIP5K*$^{-/-}$ cells) until 80-90% confluent. To harvest, dishes were quickly washed twice with cold PBS, then incubated with 1-5 mL cold 1 M perchloric acid on ice for 10 min. Acidic extracts were then collected from the plates, and inositol phosphates and other small polar molecules extracted using titanium dioxide beads[23,44]. To determine protein concentrations, post-extraction dishes were washed twice in PBS and proteins were solubilized via addition of 1.5 mL cell lysis buffer (0.1 % SDS in 0.1 M NaOH) followed by incubation for 15 min at room temperature. Cell extracts were then pelleted. Protein contents of cell lysates were determined

using the DC protein assay (Biorad) with BSA as calibration standard. To provide cell volume values and cell counts for normalization, parallel dishes were prepared and trypsinized.
For SIL-CE-ESI-MS, cells were seeded into 6 well plates. After 24 h, the medium was removed, cells were washed, then 2 mL treatment medium was added. Cells were harvested by trypsinization to maximize yield, before extraction with perchloric acid and TiO_2 beads. Parallel dishes were prepared to provide cell counts and protein concentration values for normalization.

Plants:

Arabidopsis seeds were surface sterilized and sown onto half-strength Murashige and Skoog (MS) medium supplemented with 1% succrose[34]. Plants were grown under 16h/8h day/night conditions at 22°C/20°C for 14 days. Light was provided by white LEDs ("True daylight", Polyklima). Shoots (150-180 mg, fresh weight) were shock-frozen in liquid nitrogen, homogenized and immediately resuspended in 1 M perchloric acid (SigmaAldrich). Titanium dioxide purification of inositol phosphates was carried out as described above.

D. discoideum

Wild type amoeba *D. discoideum* AX2, obtained from the Dicty Stock Center (Northwestern University, Chicago, USA), was grown in SIH defined minimal media (Formedium) at 20 °C in a flask with moderate shaking to a cell density of 3-4x10^6 cells/ml. Twenty million cells were harvested by centrifugation (1 000 g; 5 min), washed in KK2 buffer (20 mM K-Phosphate buffer pH 6.8), resuspended in 500 µL ice cold perchloric acid solution (1 M perchloric acid, 5 mM EDTA) and incubated on ice for 10 min, gently mixing the cell suspension every two min. The cell suspension was centrifuged (15 000 g; 5 min at 4 °C) and the supernatant subject to TiO_2 purification as described.

S. cerevisiae:

Wild type yeast (BY4741) was grown in Complete Supplement Mixture (SCM) media (Formedium) overnight with shaking at 30°C to logarithmic phase (OD_{600}=1-3). Forty OD_{600} units were harvested by centrifugation (1 000 g; 5 min), washed with ice cold water and resuspended in 500 µL ice cold perchloric acid solution (1 M perchloric acid, 5 mM EDTA). After adding ~300 µL acid-washed glass beads (Sigma Aldrich) yeast were vigorously vortexed for 5 min at 4 °C. The lysate was centrifuged (15 000 g; 5 min at 4 °C) and the supernatant (acid extract) subject to TiO_2 purification as described.

Inositol phosphate analysis by SAX-HPLC

Analysis of InsP pathways after [^{3}H]-inositol radiolabeling was carried out as previously described[25]. Briefly, cells were seeded into 6 well plates and grown in the presence of [^{3}H]-inositol for 5 days to ~80% confluence. Treatment with NaF (10 mM) was for 1 hour. Cells were then washed with ice-cold PBS and extracted with perchloric acid, and after neutralization processed for SAX-HPLC analysis.

Western blotting

Cells were lysed in TX buffer (50 mM HEPES pH 7.4, 1 mM EDTA, 10% glycerol, 1% Triton X-100, 50 mM sodium fluoride, 5 mM sodium pyrophosphate) supplemented with protease and phosphatase inhibitor cocktails (Sigma). Lysates were cleared by centrifugation at 18,000 rpm for 5 min at 4°C, and protein concentrations measured by DC Protein Assay (Bio-Rad). Lysates were resolved using NuPAGE 4-12% bis-tris gels (Life Technologies) and proteins transferred to nitrocellulose membranes. Ponceau S solution (0.1% Ponceau S [Sigma] in 1% acetic acid) was used to confirm equal loading. Membranes were blocked for 1 hour in 5% non-fat milk in TBS-T (10 mM Tris base, 140 mM NaCl, 0.05% Tween) then blotted for the following primary antibodies at 1:100-1:1000 overnight in 3% milk: IP6K1 (HPA040825), IP6K2 (HPA070811), IPPK (HPA020603; Sigma), ISYNA1 (sc 271830), actin (sc-1616; Santa Cruz), histone H3 (ab1791; Abcam). Secondary HRP-conjugated antibodies (Sigma) were diluted in 3% milk. Signal was detected using Luminata Crescendo Western Substrate (Merck Millipore) and Amersham Hyperfilm (VWR) and a film developer.

References

1. Irvine, R. F. & Schell, M. J. Back in the water: the return of the inositol phosphates. *Nat. Rev. Mol. Cell Biol.* **2,** 327–338 (2001).
2. Shears, S. B. Inositol pyrophosphates: why so many phosphates? *Adv. Biol. Regul.* **57,** 203–216 (2015).
3. Wilson, M. S. C., Livermore, T. M. & Saiardi, A. Inositol pyrophosphates: between signalling and metabolism. *Biochem. J.* **452,** 369–379 (2013).
4. Shears, S. B. Intimate connections: Inositol pyrophosphates at the interface of metabolic regulation and cell signaling. *J. Cell. Physiol.* **233,** 1897–1912 (2018).
5. Illies, C. *et al.* Requirement of inositol pyrophosphates for full exocytotic capacity in pancreatic beta cells. *Science* **318,** 1299–1302 (2007).
6. Szijgyarto, Z., Garedew, A., Azevedo, C. & Saiardi, A. Influence of inositol pyrophosphates on cellular energy dynamics. *Science* **334,** 802–805 (2011).
7. Wild, R. *et al.* Control of eukaryotic phosphate homeostasis by inositol polyphosphate sensor domains. *Science* **352,** 986–990 (2016).

8. Pisani, F. *et al.* Analysis of Dictyostelium discoideum inositol pyrophosphate metabolism by gel electrophoresis. *PloS one* **9,** e85533 (2014).

9. Laussmann, T., Reddy, K. M., Reddy, K. K., Falck, J. R. & Vogel, G. Diphospho-myo-inositol phosphates from Dictyostelium identified as D-6-diphospho-myo-inositol pentakisphosphate and D-5,6-bisdiphospho-myo-inositol tetrakisphosphate. *Biochem. J.* **322,** 31–33 (1997).

10. Wilson, M. S. C. & Saiardi, A. Importance of Radioactive Labelling to Elucidate Inositol Polyphosphate Signalling. *Top. Curr. Chem.* **375,** 14 (2017).

11. Whitfield, H. *et al.* An ATP-responsive metabolic cassette comprised of inositol tris/tetrakisphosphate kinase 1 (ITPK1) and inositol pentakisphosphate 2-kinase (IPK1) buffers diphosphosphoinositol phosphate levels. *Biochem. J.* **477,** 2621–2638 (2020).

12. Mayr, G. W. A novel metal-dye detection system permits picomolar-range h.p.l.c. analysis of inositol polyphosphates from non-radioactively labelled cell or tissue specimens. *Biochem. J.* **254,** 585–591 (1988).

13. Desfougères, Y., Wilson, M. S. C., Laha, D., Miller, G. J. & Saiardi, A. ITPK1 mediates the lipid-independent synthesis of inositol phosphates controlled by metabolism. *Proc. Natl. Acad. Sci. U.S.A.* **116,** 24551–24561 (2019).

14. Laha, D. *et al.* Arabidopsis ITPK1 and ITPK2 Have an Evolutionarily Conserved Phytic Acid Kinase Activity. *ACS Chem. Biol.* **14,** 2127–2133 (2019).

15. Liu, X., Villalta, P. W. & Sturla, S. J. Simultaneous determination of inositol and inositol phosphates in complex biological matrices: quantitative ion-exchange chromatography/tandem mass spectrometry. *Rapid Commun. Mass Spectrom.* **23,** 705–712 (2009).

16. Ito, M. *et al.* Hydrophilic interaction liquid chromatography-tandem mass spectrometry for the quantitative analysis of mammalian-derived inositol poly/pyrophosphates. *J. Chromatogr. A* **1573,** 87–97 (2018).

17. Berridge, M. J., Dawson, R. M., Downes, C. P., Heslop, J. P. & Irvine, R. F. Changes in the levels of inositol phosphates after agonist-dependent hydrolysis of membrane phosphoinositides. *Biochem. J.* **212,** 473–482 (1983).

18. Streb, H., Irvine, R. F., Berridge, M. J. & Schulz, I. Release of Ca2+ from a nonmitochondrial intracellular store in pancreatic acinar cells by inositol-1,4,5-trisphosphate. *Nature* **306,** 67–69 (1983).

19. Losito, O., Szijgyarto, Z., Resnick, A. C. & Saiardi, A. Inositol pyrophosphates and their unique metabolic complexity: analysis by gel electrophoresis. *PloS one* **4,** e5580 (2009).

20. Buscher, B.A.P., Hofte, A.J.P., Tjaden, U.R. & van der Greef, J. On-line electrodialysis–capillary zone electrophoresis–mass spectrometry of inositol phosphates in complex matrices. *J. Chromatogr. A* **777,** 51–60 (1997).

21. Gu, C., Wilson, M. S. C., Jessen, H. J., Saiardi, A. & Shears, S. B. Inositol Pyrophosphate Profiling of Two HCT116 Cell Lines Uncovers Variation in InsP8 Levels. *PloS one* **11,** e0165286 (2016).

22. Puschmann, R., Harmel, R. K. & Fiedler, D. Scalable Chemoenzymatic Synthesis of Inositol Pyrophosphates. *Biochemistry* **58,** 3927–3932 (2019).

23. Wilson, M. S. C., Bulley, S. J., Pisani, F., Irvine, R. F. & Saiardi, A. A novel method for the purification of inositol phosphates from biological samples reveals that no phytate is present in human plasma or urine. *Open Biol.* **5,** 150014 (2015).

24. Shears, S. B. Understanding the biological significance of diphosphoinositol polyphosphates ('inositol pyrophosphates'). *Bioche. Soc. Symp.* 211–221 (2007).

25. Azevedo, C. & Saiardi, A. Extraction and analysis of soluble inositol polyphosphates from yeast. *Nat. Protoc.* **1,** 2416–2422 (2006).

26. Wilson, M. S., Jessen, H. J. & Saiardi, A. The inositol hexakisphosphate kinases IP6K1 and -2 regulate human cellular phosphate homeostasis, including XPR1-mediated phosphate export. *J. Biol. Chem.* **294,** 11597–11608 (2019).

27. Menniti, F. S., Miller, R. N., Putney, J. W., JR & Shears, S. B. Turnover of inositol polyphosphate pyrophosphates in pancreatoma cells. *J. Biol. Chem.* **268,** 3850–3856 (1993).

28. Gu, C. *et al.* Inhibition of Inositol Polyphosphate Kinases by Quercetin and Related Flavonoids: A Structure-Activity Analysis. *J. Med. Chem.* **62,** 1443–1454 (2019).

29. Harmel, R. K. *et al.* Harnessing ^{13}C-labeled myo-inositol to interrogate inositol phosphate messengers by NMR. *Chem. Sci.* **10,** 5267–5274 (2019).

30. Desai, M. *et al.* Two inositol hexakisphosphate kinases drive inositol pyrophosphate synthesis in plants. *Plant J.* **80,** 642–653 (2014).

31. Dong, J. *et al.* Inositol Pyrophosphate $InsP_8$ Acts as an Intracellular Phosphate Signal in Arabidopsis. *Mol. Plant* **12,** 1463–1473 (2019).

32. Saiardi, A., Caffrey, J. J., Snyder, S. H. & Shears, S. B. Inositol polyphosphate multikinase (ArgRIII) determines nuclear mRNA export in Saccharomyces cerevisiae. *FEBS Lett.* **468,** 28–32 (2000).

33. Nagy, R. *et al.* The Arabidopsis ATP-binding cassette protein AtMRP5/AtABCC5 is a high affinity inositol hexakisphosphate transporter involved in guard cell signaling and phytate storage. *J. Biol. Chem.* **284,** 33614–33622 (2009).

34. Laha, D. *et al.* VIH2 Regulates the Synthesis of Inositol Pyrophosphate InsP8 and Jasmonate-Dependent Defenses in Arabidopsis. *Plant Cell* **27,** 1082–1097 (2015).

35. Laussmann, T., Eujen, R., Weisshuhn, C. M., Thiel, U. & Vogel, G. Structures of diphospho-myo-inositol pentakisphosphate and bisdiphospho-myo-inositol tetrakisphosphate from Dictyostelium resolved by NMR analysis. *Biochem. J.* **315,** 715–720 (1996).

36. Capolicchio, S., Thakor, D. T., Linden, A. & Jessen, H. J. Synthesis of unsymmetric diphospho-inositol polyphosphates. *Ange. Chem. Int. Ed.***52,** 6912–6916 (2013).

37. Capolicchio, S., Wang, H., Thakor, D. T., Shears, S. B. & Jessen, H. J. Synthesis of densely phosphorylated bis-1,5-diphospho-myo-inositol tetrakisphosphate and its enantiomer by bidirectional P-anhydride formation. *Ange. Chem. Int. Ed.* **53,** 9508–9511 (2014).

38. Pavlovic, I., Thakor, D. T. & Jessen, H. J. Synthesis of 2-diphospho-myo-inositol 1,3,4,5,6-pentakisphosphate and a photocaged analogue. *Org. Biomol. Chem.* **14,** 5559–5562 (2016).

39. Leung, K.-Y., Mills, K., Burren, K. A., Copp, A. J. & Greene, N. D. E. Quantitative analysis of myo-inositol in urine, blood and nutritional supplements by high-performance liquid chromatography tandem mass spectrometry. *J. chromatogr. B* **879,** 2759–2763 (2011).

40. Shears, S. B. Assessing the omnipotence of inositol hexakisphosphate. *Cell. Signal.* **13,** 151–158 (2001).

41. Ju, S., Shaltiel, G., Shamir, A., Agam, G. & Greenberg, M. L. Human 1-D-myo-inositol-3-phosphate synthase is functional in yeast. *J. Biol. Chem.* **279,** 21759–21765 (2004).

42. Dovey, C. M. *et al.* MLKL Requires the Inositol Phosphate Code to Execute Necroptosis. *Mol. Cell* **70,** 936-948.e7 (2018).

43. Gu, C. *et al.* KO of 5-InsP$_7$ kinase activity transforms the HCT116 colon cancer cell line into a hypermetabolic, growth-inhibited phenotype. *Proc. Natl. Acad. Sci. U.S.A.* **114,** 11968–11973 (2017).

44. Wilson, M. S. & Saiardi, A. Inositol Phosphates Purification Using Titanium Dioxide Beads. *Bio Protoc.* **8** (2018).

45. Orellana, E. A. & Kasinski, A. L. Sulforhodamine B (SRB) Assay in Cell Culture to Investigate Cell Proliferation. *Bio Protoc.* **6** (2016).

Figures & legends

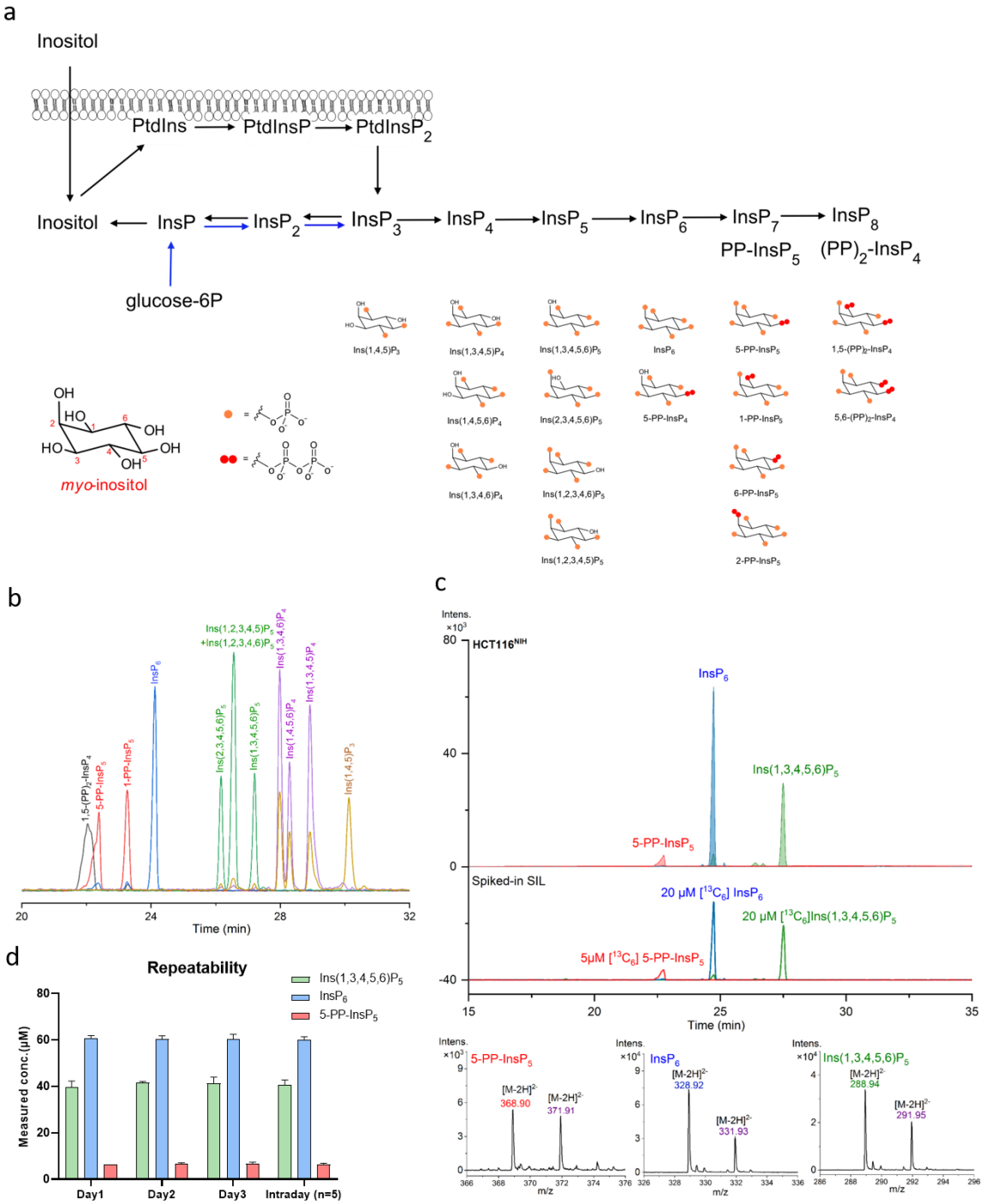

Figure 1 **Separation of PP-InsP and InsP by CE-ESI-MS. (a)** Simplified biosynthesis of inositol phosphate (InsPs) and inositol pyrophosphates (PP-InsPs) from lipid $PInsP_2$ and glucose-6P, with the structures of InsPs and PP-InsPs that can be currently resolved by CE-ESI-MS. The metabolic pathways for inositol (pyro)phosphates in mammals are shown in Supplementary Fig. 1; **(b)** Separation of PP-InsP and InsP standards by CE-ESI-MS. BGE: 35 mM ammonium acetate titrated with ammonium hydroxide to pH 9.7, CE voltage: 30 kV, CE current: 23 μA, injection: 50 mbar, 10 s (10 nL), solutes: 5 μM for $Ins(2,3,4,5,6)P_5$, $Ins(1,3,4,5,6)P_5$, $Ins(1,2,3,4,6)P_5$, $Ins(1,2,3,4,5)P_5$, $InsP_6$, 5-PP-$InsP_5$, 1-PP-$InsP_5$ and 1,5-

$(PP)_2$-InsP_4, 20 µg/mL for Ins(1,3,4,5)P_4 and Ins(1,3,4,6)P_4, 8 µg/mL for Ins(1,4,5,6)P_4 and 10 µg/mL for Ins(1,4,5)P_3; **(c)** Extracted ion electropherograms (EIEs) of the main inositol (pyro)phosphates in HCT116^{NIH} and spiked stable isotopic labelled (SIL) internal standards 20 µM [$^{13}C_6$]Ins(1,3,4,5,6)P_5, 20 µM [$^{13}C_6$]InsP_6 and 5 µM [$^{13}C_6$] 5-PP-InsP_5. The InsP species Ins(1,3,4,5,6)P_5, InsP_6, and 5-PP-InsP_5 in HCT116^{NIH} were assigned by their accurate mass, and identical migration time with spiked SIL standards; **(d)** Intra- and interday repeatability of the inositol (pyro)phosphate analysis by CE-ESI-MS; error bars represent the standard deviation, n=5.

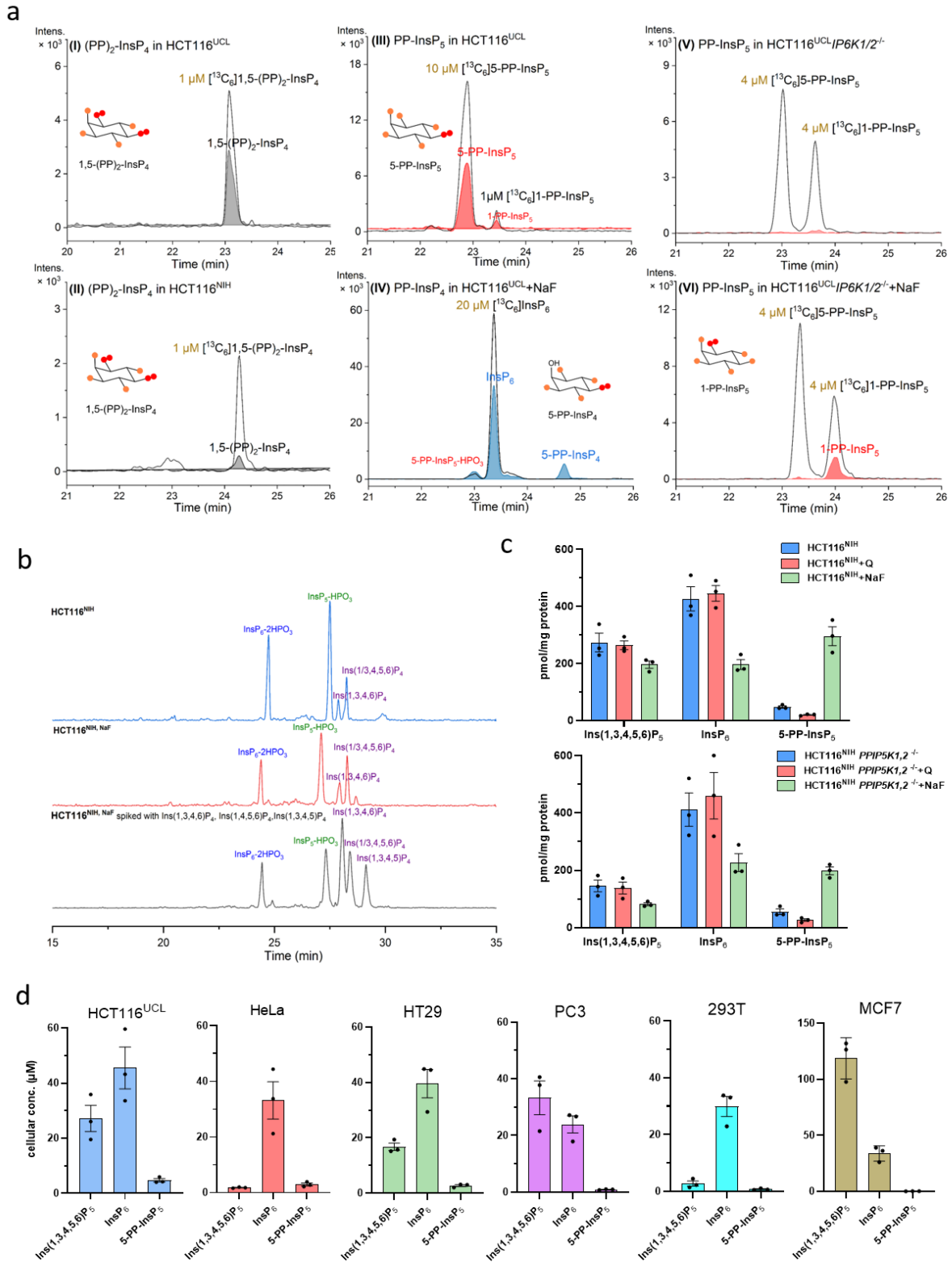

Figure 2. **CE-ESI-MS analysis of mammalian PP-InsP and InsP metabolism. (a)** Mammalian cell extracts were analysed by CE-ESI-MS after spiking the indicated amount (yellow) of stable isotopic standard. Extracted ion electropherograms of 1,5-$(PP)_2$-$InsP_4$ in $HCT116^{UCL}$ (I) and $HCT116^{NIH}$ (II) spiked with $[^{13}C_6]$ 1,5-$(PP)_2$-$InsP_4$, (III) PP-$InsP_5$ in $HCT116^{UCL}$, major 5-PP-$InsP_5$ and minor 1-PP-$InsP_5$, (IV) 5-PP-$InsP_4$ in $HCT116^{UCL}$ cells with

NaF treatment, (V) no measurable PP-InsP$_5$ in HCT116^{UCL}*IP6K1,2*$^{-/-}$, (VI) 1-PP-InsP$_5$ is detectable in HCT116^{UCL}*IP6K1,2*$^{-/-}$ cells after 1 h sodium fluoride (NaF) treatment; **(b)** analysis of InsP$_4$ isomers in HCT116^{NIH}, HCT116^{NIH,NaF} and HCT116^{NIH,NaF} spiked with Ins(1,3,4,6)P$_4$ (2 µg/mL), Ins(1,4,5,6)P$_4$ (1 µg/mL) and Ins(1,3,4,5)P$_4$ (2 µg/mL); **(c)** Inositol (pyro)phosphate levels in HCT116^{NIH} and HCT116^{NIH}*PPIP5K1,2*$^{-/-}$ cells, without treatment or after incubation with NaF or inositol polyphosphate kinase (IPMK) inhibitor quercetin (2.5 µM for 30 min). Bars are means ± SEM from three independent experiments, individual values are shown by dots; **(d)** Cellular concentration of InsPs in the immortal human cell lines HCT116^{UCL}, HeLa, HT29, 293T, PC3, and MCF7. Concentrations varying between 2-120 µM Ins(1,3,4,5,6)P$_5$, 24-46 µM InsP$_6$ and 0-5 µM 5-PP-InsP$_5$ were found. Data are means ± SEM from three independent experiments. InsP levels normalized by protein content among these cells are shown in Supplementary Fig. 4.

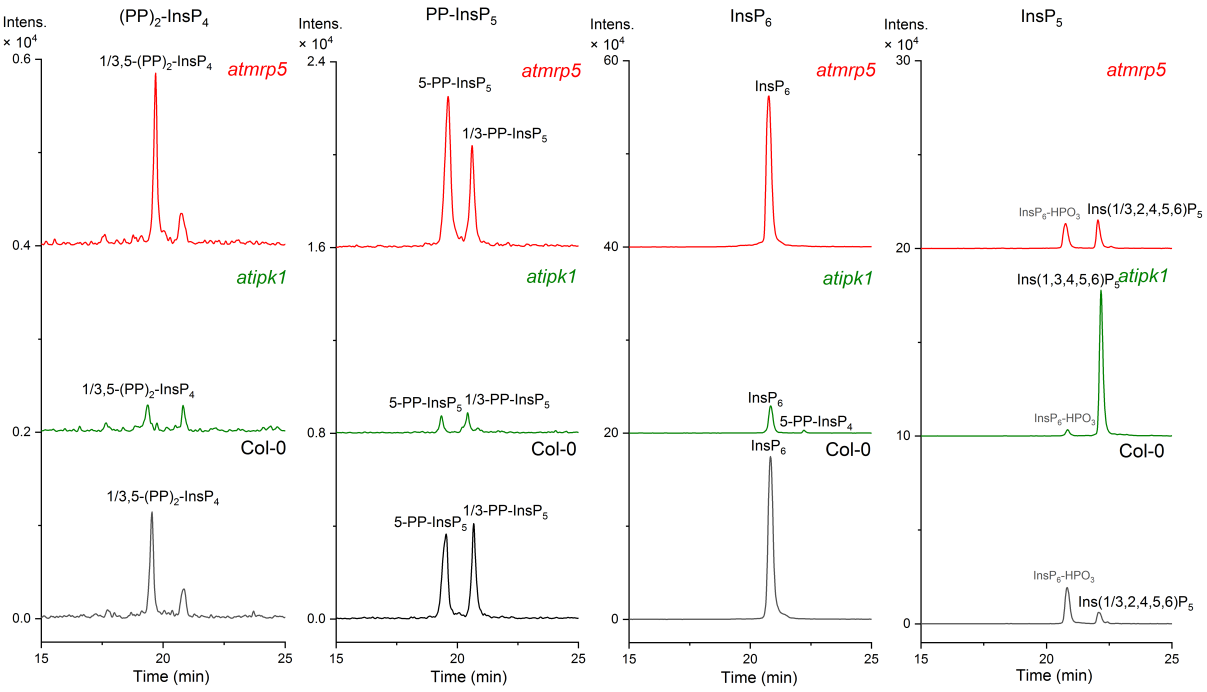

Figure 3 **CE-ESI-MS analysis of PP-InsP in *Arabidopsis thaliana* shoots. Shoot** extracts from wild type (Col-0), *atipk1* and *atmrp5* mutant plants were analysed to assess the presence of $InsP_5$, $InsP_6$, 5-PP-$InsP_5$, and 1,5-$(PP)_2$-$InsP_4$. $InsP_5$ isomer composition differed in the different genotypes: Ins(1/3,2,4,5,6)P_5 is present in Col-0 and the *mrp5* mutant, whereas Ins(1,3,4,5,6)P_5 was detected in *atipk1* plants. A decreased level of 1,5-$(PP)_2$-$InsP_4$, 5-PP-$InsP_5$, 1-PP-$InsP_5$, $InsP_6$, and increased level of 5-PP-$InsP_4$ and Ins(1,3,4,5,6)P_5 were observed for the *atipk1* mutant. In the *atmrp5* mutant, levels of 1,5-$(PP)_2$-$InsP_4$ and 5-PP-$InsP_4$ were increased. The electropherograms are representative of independent biological duplicates giving comparable results.

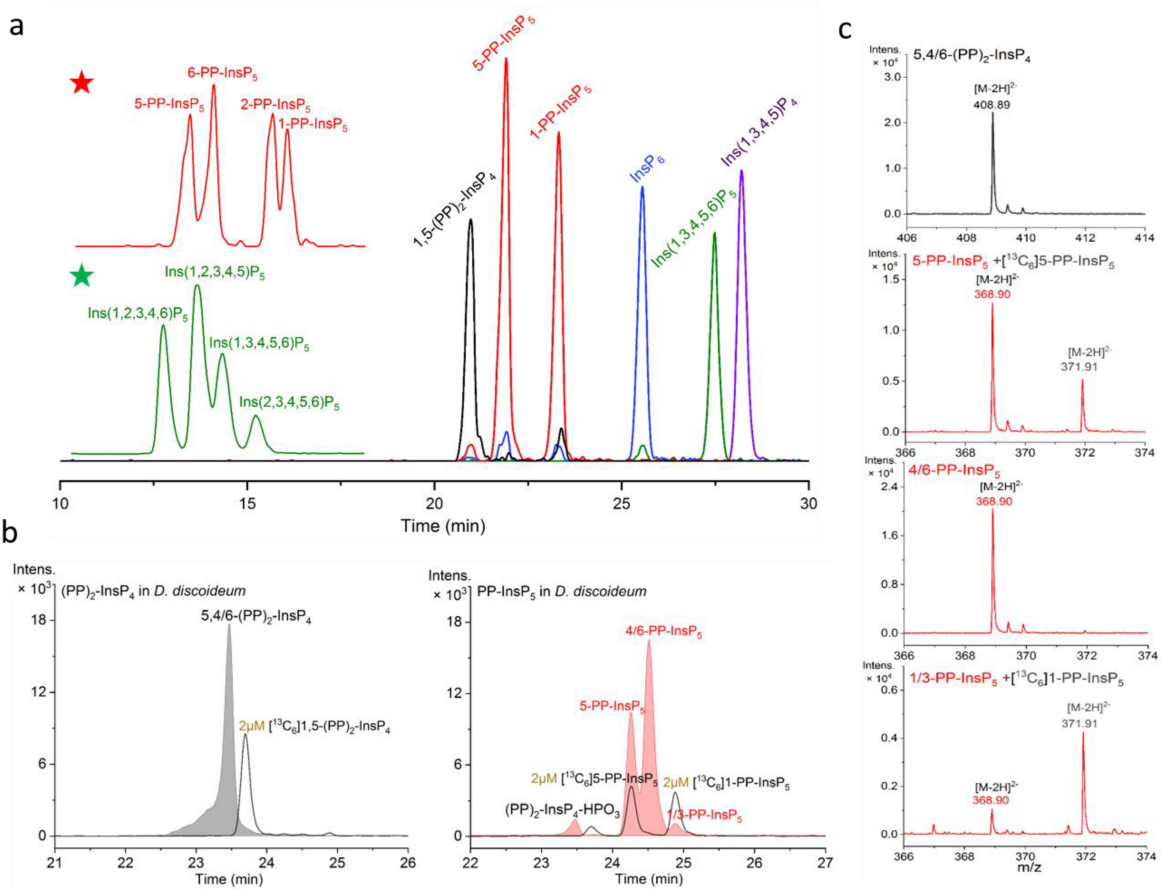

Figure 4 **CE-ESI-MS analysis of *Dictyostelium discoideum* extract. (a)** Separation of PP-InsP and InsP standards using a modified BGE (30 mM ammonium acetate titrated with NH_4OH to pH 9.0). Enlarged inserts for PP-InsP_5 (★) and InsP_5 (★) reveal the separation of all regioisomers using the following parameters. CE voltage: 30 kV, CE current: 19 µA, injection: 50 mbar, 10 s (10 nL), solutes: 10 µM for Ins(1,3,4,5,6)P_5, InsP_6, 5-PP-InsP_5, 1-PP-InsP_5 and 1,5-$(PP)_2$-InsP_4, 20 µg/mL for Ins(1,3,4,5)P_4; **(b)** PP-InsPs in *D. discoideum* extracts. PP-InsP regioisomers could be efficiently assigned and quantified in single runs with spiked (isotopic) standards: major 5,4/6-$(PP)_2$-InsP_4, 4/6-PP-InsP_5 and 5-PP-InsP_5, minor 1/3-PP-InsP_5; **(c)** Mass spectra for PP-InsPs in *D. discoideum* in (b). Three independent *D. discoideum* AX2 (wild type) extracts were analyzed giving identical results.

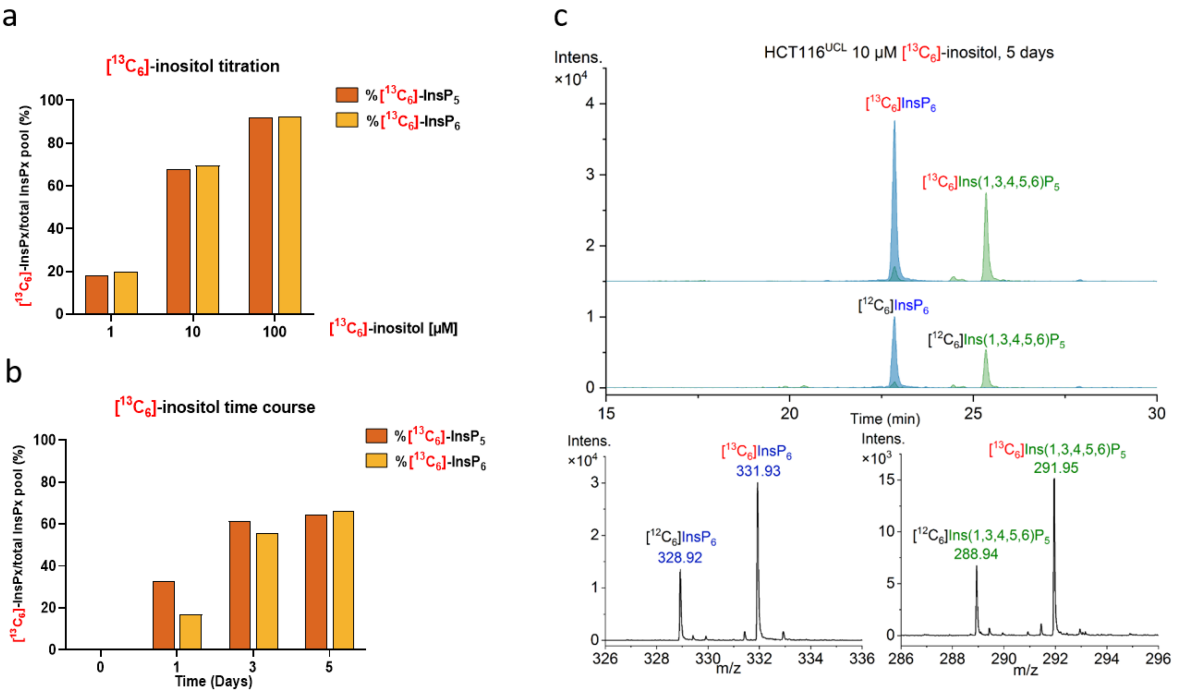

Figure 5 **CE-ESI-MS analysis after [$^{13}C_6$]-inositol labeling. (a)** Ratio of [$^{13}C_6$]InsP$_x$ (x= 5 or 6) over total InsP$_x$ ([$^{13}C_6$]InsP$_x$ + [$^{12}C_6$]InsP$_x$) pool in wild type HCT116^{UCL} after 5 days incubation with different concentrations of [$^{13}C_6$]-inositol (1,10,100 μM) in inositol-free DMEM; **(b)** Ratio of [$^{13}C_6$]-InsP$_x$ in total InsP$_x$ pool in wild type HCT116^{UCL} cells incubated with 10 μM [$^{13}C_6$]-inositol in inositol-free DMEM for 1, 3 and 5 days; **(c)** EIEs of InsP$_6$ and Ins(1,3,4,5,6)P$_5$ in HCT116^{UCL} cells after 5 days incubation with 10 μM [$^{13}C_6$]-inositol and relative mass spectra.

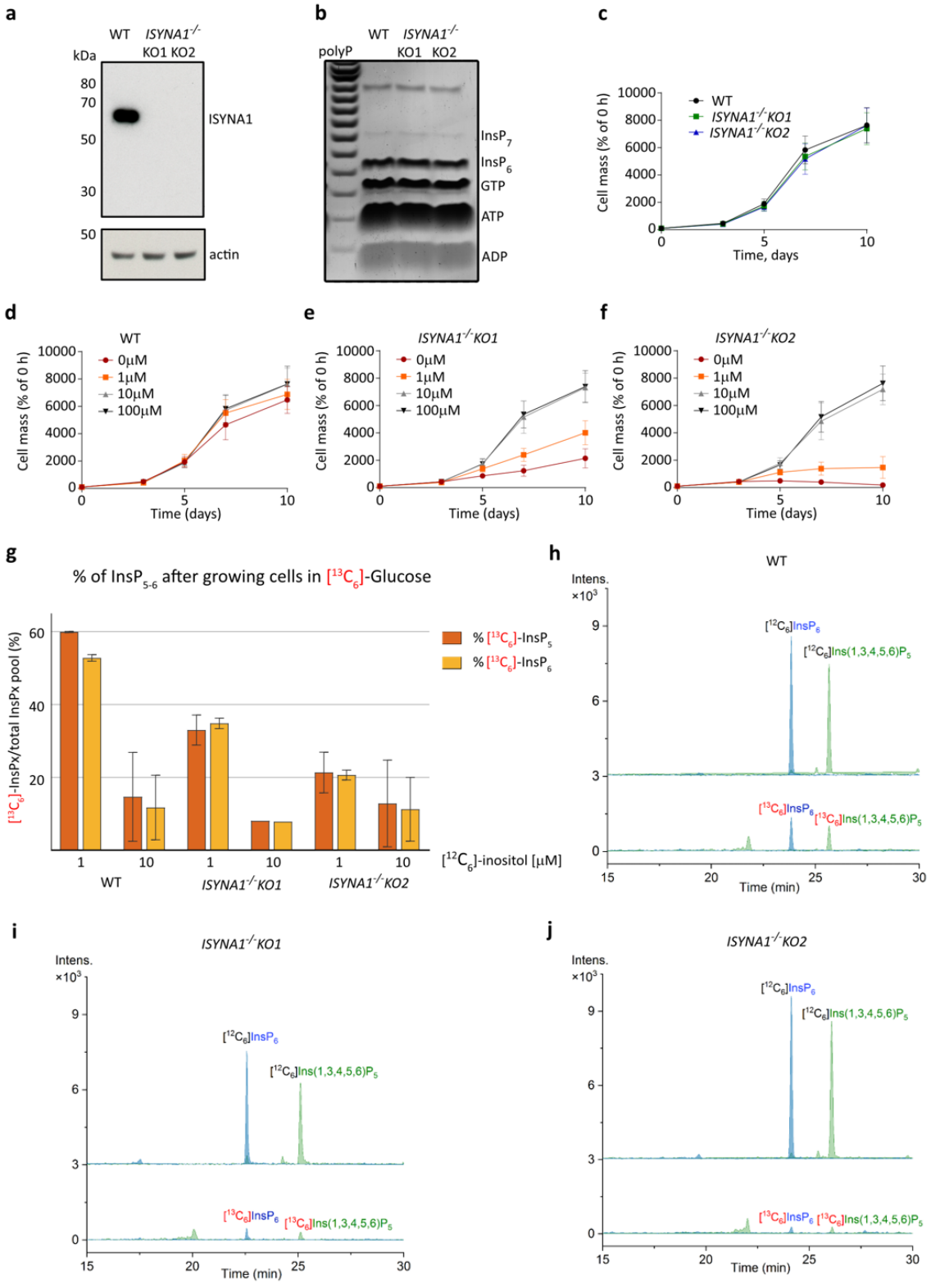

Figure 6 **Analysis of *ISYNA1*$^{-/-}$ cell lines by CE-ESI-MS. (a)** Western blot showing the absence of ISYNA1 protein in CRISPR-generated HCT116^{UCL} *ISYNA1*$^{-/-}$ clones KO1 and KO2. These lines possess a normal level of $InsP_6$ as revealed by PAGE **(b)** and a normal growth rate in standard DMEM **(c)**. Inositol titration growth curves **(d, e, f)** demonstrated strongly

reduced growth for the KO cells in the absence of inositol, while a concentration of 10 μM inositol is sufficient to restore normal growth. **(g)** Ratio of [$^{13}C_6$]$InsP_x$ over total $InsP_x$ pool (x = 5 or 6) in WT, KO1 and KO2 clones grown for 5 days in 25 mM [$^{13}C_6$]-glucose supplemented with 1 or 10 μM inositol. Data are means ± SD from two independent experiments; **(h)** EIEs of $InsP_6$ and Ins(1,3,4,5,6)P_5 in HCT116^{UCL} cells after 5 days in 25 mM [$^{13}C_6$]-glucose and 10 μM inositol, strongly supporting a pathway from glucose for the biosynthesis of inositol phosphates in mammals; **(i)&(j)** EIEs of $InsP_6$ and Ins(1,3,4,5,6)P_5 in KO1 and KO2 cells after 5 days in 25 mM [$^{13}C_6$]-glucose with 10 μM inositol. Detectable [$^{13}C_6$]$InsP_x$ was produced in both clones although at a lesser degree than in wild type (h).